# DICTRA, a Tool for Simulation of Diffusional Transformations in Alloys

*Annika Borgenstam, Anders Engstrom, Lars Hoglund, and John Agren*

*(Submitted 20 September 1999; in revised form 14 February 2000)*

**In the present paper, a general survey of the diffusion-controlled transformations (DICTRA) software is given. DICTRA is an engineering tool for diffusion simulations in multicomponent alloys. The simulations are based on multicomponent diffusion and thermodynamic data, both obtained by analyzing and assessing experimental information. This allows for many different cases to be studied as soon as the underlying data are available. DICTRA is not a complete simulation tool because only geometries that can be transformed into one space variable can be treated, but many well posed problems of practical interest may be solved. The program contains several different models, which are discussed in the present paper. Each model has its own applications and several examples from recent simulations are given in order to demonstrate the usage of the particular models.**

## 1. Introduction

Mathematical modeling of various physical processes and simulation thereof has become a necessity for the materials engineer. The simulation allows important issues to be studied, involving, *e.g.*, design and optimization of material properties. Previously, such modeling was mostly analytical or empirical and usually many simplifying assumptions had to be made in order to allow such treatment. The development of improved computer resources, which has occurred during the last decades, and the desire to tackle more difficult problems have resulted in an increasing use of numerical methods in the field of computational materials science. Today, the computers are powerful enough, and many of the developed software packages are advanced enough, to handle problems of industrial importance, *i.e.*, problems involving "real" alloys.

To be able to simulate diffusion-controlled transformations, a tool to calculate thermodynamic quantities and a tool to treat the kinetics of the transformations are needed. More than 25 years ago, the development of a software for all kinds of thermodynamic and phase diagram calculations, Thermo-Calc [1985Sun], started at the Royal Institute of Technology in Stockholm. This software has been quite successful; *e.g.*, it can predict the correct equilibrium states in real alloys containing more than ten alloying elements [1997Sau]. Later, in the same group, work was initiated in order to treat nonequilibrium processes [1982Ågr2], and this was the starting point of the diffusion-controlled transformations (DICTRA) software [1990And].

Today, DICTRA constitutes a flexible software for simulation of diffusion-controlled transformations in multicomponent alloys and has been used successfully to simulate complex systems, *e.g.*, heat treatments of multicomponent alloys [1997Hög]. However, the DICTRA software can only handle simple geometries, and thus, it is not a complete simulation tool. The geometries that can be handled are planar, cylindrical, and spherical, of which all can be reduced into one space variable. The planar geometry is an infinitely wide plate of a certain width, the cylindrical geometry is an infinitely long cylinder of a certain radius, and the spherical geometry is a sphere with a certain radius. Using these geometries, the software can be used to solve certain well-defined problems very accurately.

The accuracy of DICTRA simulations is highly dependent on the accuracy of the thermodynamic and kinetic data used but also on different assumptions, such as choice of geometry. The best way to check the accuracy is to compare the simulation with experimental data. This will be done for several different simulations in this paper.

The purpose of the present paper is to briefly describe the use and limitations of the different models, which constitute the DICTRA software, as well as to demonstrate the potential use of DICTRA as an engineering tool. The latter is accomplished by showing simulation results from several recent DICTRA applications.

It can here be mentioned that multicomponent diffusion problems have been tackled by several authors over the years. For example, carburization in a multicomponent system has been modeled by Bongartz *et al.* [1980Bon, 1989Bon] and also by Morral *et al.* [1992Mor]. Kattner *et al.* have modeled solidification in multicomponent alloys [1996Kat], Lee has presented a model for simulation of diffusional reactions between multiphase alloys with different matrix phases [1999Lee], and Reed *et al.* have modeled the formation of sigma phase [1999Ree].

## 2. Multicomponent Diffusion Theory

In the presence of a concentration gradient, a net flux of the corresponding species is established. The law relating flux and concentration gradient is Fick's first law, which, in

**Annika Borgenstam, Lars Höglund,** and **John Ågren,** Division of Physical Metallurgy, Royal Institute of Technology, Stockholm SE-100 44, Sweden. **Anders Engström** is at AB Sandvik Hard Materials, SE-126 80, Stockholm, Sweden.

the case of an isothermal, isobaric one-phase binary alloy with diffusion of species $k$ in one direction $z$, is expressed as

$$J_k = -D_k \frac{\partial c_k}{\partial z} \quad \text{(Eq 1)}$$

where $J_k$ is the interdiffusion flux, *i.e.*, the amount of diffusing substance that passes per unit time and unit area of a plane perpendicular to the $z$-axis, defined with respect to the volume-fixed or Matano frame of reference. $c_k$ is the concentration of $k$, *i.e.*, the amount of the diffusing substance per unit volume. $D_k$ is the diffusivity or the interdiffusion coefficient of species $k$ and depends generally on concentration and temperature.

By itself, Fick's first law is not very useful. However, when combined with the continuity equation,

$$\frac{\partial c_k}{\partial t} = \frac{\partial}{\partial z}(-J_k) \quad \text{(Eq 2)}$$

it gives the fundamental differential equation of diffusion,

$$\frac{\partial c_k}{\partial t} = \frac{\partial}{\partial z}\left(D_k \frac{\partial c_k}{\partial z}\right) \quad \text{(Eq 3)}$$

usually referred to as Fick's second law.

Most alloys contain more than two species. In such cases, it is found that the diffusivities in Eq 1 do not only depend on concentration but also on the concentration gradients. This makes Eq 1 rather useless for practical calculations in multicomponent alloys. The multicomponent extension to Fick's first law was first expressed by Onsager [1931Ons]. He postulated that each thermodynamic flux was linearly related to every thermodynamic force, and thus, in the case of diffusion of mass in the $z$ direction for an isothermal isobaric system, we have

$$J_k = -\sum_{i=1}^{n} L'_{ki} \frac{\partial \mu_i}{\partial z} \quad \text{(Eq 4)}$$

The $\mu_i$ terms are the chemical potentials for the various species and may be assumed to be unique functions of the composition, *i.e.*, $\mu_i = f(c_1, c_2, c_3, \ldots c_n)$. The term $L'_{ki}$ here can be considered as the proportionality factor, which depends on the mobility of the individual species, which will be discussed further in Section 3. The flux $J_k$ is defined in such a way

$$\sum_{k=1}^{n} V_k J_k = 0 \quad \text{(Eq 5)}$$

where the summation is performed over all elements. Generally, it is much more convenient to express the fluxes as functions of gradients in concentration rather than gradients in chemical potential. This is accomplished by rewriting Eq 4 using the chain role of derivation, *i.e.*,

$$J_k = -\sum_{i=1}^{n} L'_{ki} \sum_{j=1}^{n} \frac{\partial \mu_i}{\partial c_j} \frac{\partial c_j}{\partial z} \quad \text{(Eq 6)}$$

or equally if the unreduced diffusivities, $D_{kj}$, are introduced,

$$J_k = -\sum_{j=1}^{n} D_{kj} \frac{\partial c_j}{\partial z} \quad \text{(Eq 7)}$$

and we may thus identify

$$D_{kj} = -\sum_{i=1}^{n} L'_{ki} \frac{\partial \mu_i}{\partial c_j} \quad \text{(Eq 8)}$$

The $\partial \mu_i / \partial c_j$ values are purely thermodynamic quantities, sometimes referred to as thermodynamic factors. It is thus evident that the diffusivities may be looked upon as consisting of two separate parts, one purely thermodynamic and one kinetic.

The $n$ concentration gradients in Eq 7 are not independent and, for practical calculations, one usually eliminates one of them. The reduced diffusivities in a volume-fixed frame of reference, where it is assumed that all the substitutional species have the same partial molar volumes, and furthermore, only the substitutional species contribute to the volume, is expressed as

$$D^n_{kj} = D_{kj} - D_{kn} \text{ (when } j \text{ is substitutional)} \quad \text{(Eq 9a)}$$

$$D^n_{kj} = D_{kj} \text{ (when } j \text{ is interstitial)} \quad \text{(Eq 9b)}$$

where the concentration gradient of $n$ has been eliminated. Using these diffusivities, Eq 7 now becomes

$$J_k = -\sum_{j=1}^{n-1} D^n_{kj} \frac{\partial c_j}{\partial z} \quad \text{(Eq 10)}$$

This equation includes the possibility that the concentration gradient of one species may cause another species to diffuse, which was suggested by Darken [1942Dar] back in 1942, and later experimentally verified by him [1949Dar]. In that experiment, two Fe-Si-C steels with similar carbon content, but with different silicon content, were welded together and annealed. Darken observed that carbon diffused from low C to high C concentrations, so-called "up hill" diffusion.

If Eq 10 is combined with Eq 2, we finally arrive at a system of coupled partial differential equations (PDEs), which is suitable for practical calculations in multicomponent alloys. If all the coefficients $D^n_{kj}$ are constant, it is sometimes possible to find analytical solutions [1971Gup], but in general, numerical methods must be applied as done by Ågren [1982Ågr2] and as used in DICTRA.

## 3. Thermodynamic and Kinetic Basis

From the preceding paragraph, it is evident that in order to perform simulations using the DICTRA software, it is

necessary that both thermodynamic and kinetic data are available. Moreover, the results and the accuracy of these simulations critically depend on the quality of these data.

Thermodynamic data have been used in order to calculate phase diagrams for more than 25 years now. One method, which has proven very powerful, is the calculation of phase diagrams (CALPHAD) method [1996Ågr], established by the pioneering work of Kaufman and Bernstein [1970Kau] in the early 1970s. In this method, the Gibbs energy of the individual phases is modeled as a function of temperature, composition, and sometimes pressure. Having this information, the equilibrium is simply calculated by an energy minimization procedure.

The Gibbs energy models in the CALPHAD method contain thermodynamic parameters, which are evaluated from the available thermodynamic information. Nowadays, the evaluation is usually made on a computer where the optimum set of parameters is found by minimizing the sum of the squares of difference between experimental and calculated values. The most commonly used optimization programs are the PARROT program [1984Jan] included in the Thermo-Calc system [1985Sun] and the Bingss and Tergss programs by Lukas [1977Luk]. The assessment of experimental information and the evaluation of model parameters to be entered into the databases are quite time consuming, and even for an expert, it may take half a year to evaluate a complex binary system. However, due to the collaboration between different European groups within the Scientific Group Thermodata Europe (SGTE) [1994SGT] over the last years, some fairly substantial thermodynamic databases have been established.

Inspired by the CALPHAD method, Andersson and Ågren [1992And] suggested a similar method for calculating kinetic data. They chose to represent the atomic mobility of the individual species in a multicomponent solution phase as a function of temperature, pressure, and composition. From absolute-reaction rate theory arguments, they divided the mobility coefficient for element B, $M_B$, into a frequency factor $M_B^\circ$ and an activation enthalpy $Q_B$; *i.e.*,

$$M_B = \frac{M_B^\circ}{RT} \exp\left(\frac{-Q_B}{RT}\right) \qquad \text{(Eq 11)}$$

where R is the gas constant and $T$ is the absolute temperature. Both $M_B^\circ$ and $Q_B$ will, in general, depend upon composition, temperature, and pressure. In the spirit of the CALPHAD approach, Andersson and Ågren represented the composition dependency as a linear combination of the values at each endpoint of the composition space and a Redlich-Kister expansion,

$$\Phi_B = \sum_i x_i \Phi_B^i + \sum_i \sum_{j>1} x_i x_j \left[\sum_{r=0}^{m} {}^r\Phi_B^{i,j}(x_i - x_j)^r\right] \qquad \text{(Eq 12)}$$

where $\Phi_B$ represents ln $M_B^\circ$ or $Q_B$. The term $\Phi_B^i$ is the value of $\Phi_B$ for pure $i$ and thus represents one of the endpoint values in the composition space. The term ${}^r\Phi_B^{i,j}$ represents binary interaction parameters, the commas separating different species interacting with each other. The terms $x_i$ and $x_j$ are mole fractions for elements $i$ and $j$, respectively.

As in the case when evaluating thermodynamic data, the model parameters, *i.e.*, $\Phi_B^i$, ${}^r\Phi_B^{i,j}$, *etc.*, are determined by an optimization procedure where experimental information is taken into account; refer to the works by Jönsson [1994Jön1, 1994Jön2, 1995Jön] and Engström and Ågren [1996Eng1].

The reason to store the individual mobilities in the database, rather than the interdiffusion coefficients, is that in an $n$-component system, there are $n$ mobilities and $(n - 1)^2$ interdiffusion coefficients, and thus, for systems with more than two components, there are fewer mobilities than diffusivities that need to be stored. The interdiffusion coefficients can always be calculated from the mobilities if the thermodynamic factors are known. The thermodynamic factors are essentially second derivatives of the molar Gibbs energy with respect to concentration and are thus known if the thermodynamic description of the system has been evaluated.

The mobilities are related to the interdiffusion coefficients by Eqs 8, 9a, 9b, and the following equation:

$$L'_{kj} = \sum_{i=1}^{n} (\delta_{ik} - c_k V_i) c_i y_{va} M_i \qquad \text{(Eq 13)}$$

where $\delta_{ik}$ is the Kronecker delta; *i.e.*, $\delta_{ik} = 1$ when $j = k$ and $\delta_{ik} = 0$ otherwise. The terms $c_k$ and $c_i$ are the amounts of $k$ and $i$ per unit volume, $V_i$ is the partial molar volume of element $i$, and $y_{va}$ is the fraction of vacant lattice sites on the sublattice where $i$ is dissolved. The term $M_i$ is the mobility of $i$ when $i$ is an interstitial and the mobility divided by $y_{va}$ when $i$ is substitutionally dissolved. The term $L_{kj}$ is defined by Eq 4.

## 4. DICTRA Models and Applications

The DICTRA software is the result of many years of ongoing development at the Royal Institute of Technology in Stockholm and Max Planck Institut für Eisenfurschung in Düsseldorf. There are several different models within DICTRA and each model has its own applications:

- single-phase model,
- moving boundary model,
- model for diffusion in dispersed systems,
- "effective" diffusion model,
- "cell" model,
- model for coarsening, and
- cooperative growth model.

A brief description of the models and some examples of their applications will be given below.

### 4.1 Single-Phase Model

The single-phase model is the most basic model. Equation 2 is solved in one phase applying a numerical procedure for

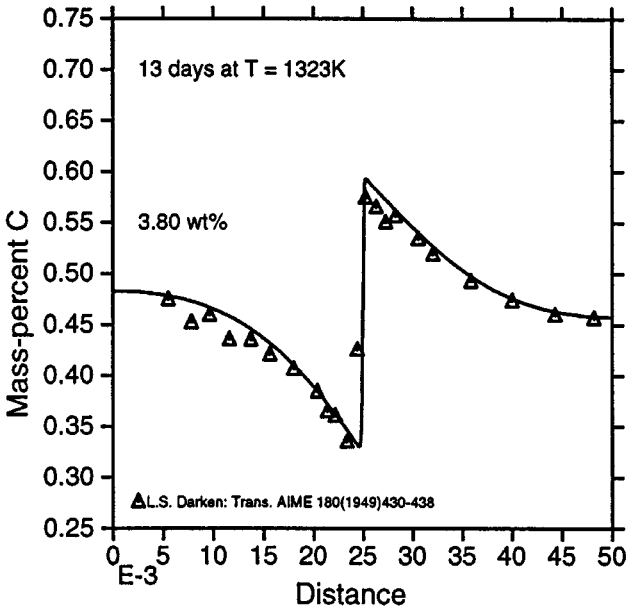


**Fig. 1** Calculated C-concentration profile in a weld between two steels with initially similar C contents, 0.49 and 0.45%, but with different silicon contents, 3.8 and 0.05%, respectively

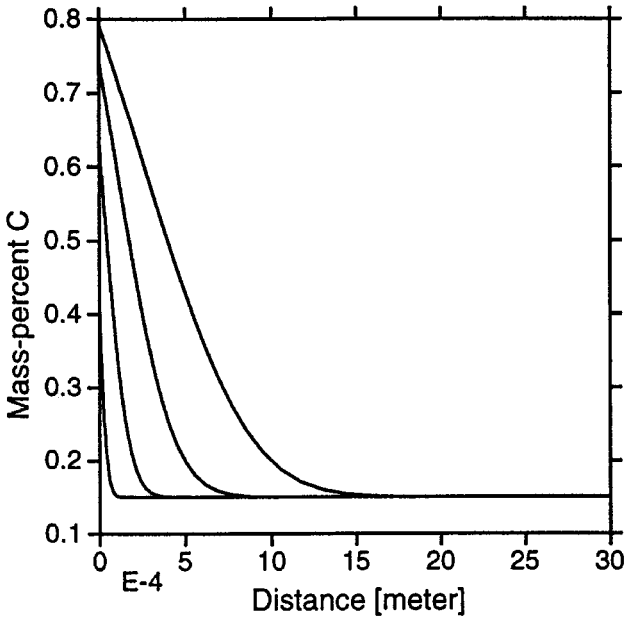


**Fig. 2** Calculated C-concentration profiles after 100, 1000, 5000, and 18,000 s at 900 °C in a carburizing atmosphere. The C flux at the surface was calculated as $J_C = 8.25 \cdot 10^{-9}(0.64 - a_C^{surface})$, where $8.25 \cdot 10^{-9}$ is a mass-transfer coefficient and 0.64 is the carbon activity of the surrounding atmosphere

a system of coupled parabolic partial differential equations [1982Ågr2]. The numerical procedure is based on the Galerkin method for space discretization [1977Zie] and the Gaussian elimination technique with incomplete factorization for solving the algebraic equations. Time integration can be chosen to be implicit, explicit, or trapezoidal. The procedure can well handle nonlinearities caused by a varying diffusion-coefficient matrix or nonlinear boundary conditions. Boundary conditions of many different kinds may be applied in a flexible way. Below is given an example with a surface reaction represented by a flux as a function of the activity at the surface. Other boundary conditions can include a state variable expression or a fixed value of the flux.

Some typical applications of this model are

- homogenization of alloys [1998Lip] and
- carburizing and decarburizing of steels [1998Spr].

**Uphill Diffusion in an Fe-Si-C Alloy.** This example comes from the well-known Darken experiment [1949Dar] previously mentioned. Two alloys with similar C contents, 0.49 and 0.45 mass.%, but different Si contents, 3.8 and 0.05 mass.%, respectively, are joined and annealed at 1050 °C in the austenitic state. Since Si diffuses much slower than C and also increases the C activity, C will diffuse from the side with high Si content to the side with low Si content, up its own concentration gradient, so-called uphill diffusion. The C concentration profile at a time when almost no diffusion of Si has occurred is shown in Fig. 1. The symbols denote the experimental measurements by Darken.

**Carburizing with Surface Reaction.** During carburization of steel in a mixture of 40% $N_2$ and 60% cracked methanol, the C activity at the steel surface is determined by a surface reaction. The C flux at the boundary may then be represented by an expression such as

$$J_C = f_C(a_C^{gas} - a_C^{surface}) \tag{14}$$

where $a_C^{gas}$ is the carbon activity of the gas and $a_C^{surface}$ is the actual carbon activity in the steel very close to the surface. The term $f_C$ is the so-called mass-transfer coefficient and may depend on both temperature and gas composition. Simulated C-concentration profiles in an Fe-0.15 mass.% C alloy when the carbon activity of the gas is 0.64, relative to graphite, and the calculated mass-transfer coefficient is $8.25 \cdot 10^{-9}$ mol/s, are shown in Fig. 2. The mass increase (per unit area) due to the carburization as a function of time is shown in Fig. 3.

### *4.2 Moving Boundary Model*

The moving boundary model treats problems where diffusion causes a phase transformation, *e.g.*, growth or dissolution of individual particles in a matrix [1992Ågr]. In the model, two single-phase regions are separated by a planar boundary and the boundary migration is determined by the rate of diffusion to and from the interface.

Consider the phase transformation between a phase $\alpha$ and its adjacent phase $\beta$ (Fig. 4). In order to conserve the number of moles of a component $k$, a flux balance equation can be formulated as

$$\frac{\nu^\alpha}{V_m^\alpha}[x_k^\alpha - x_k^\beta] = J_k^\alpha - J_k^\beta \quad k = 1,2 \ldots n-1 \qquad \text{(Eq 15)}$$

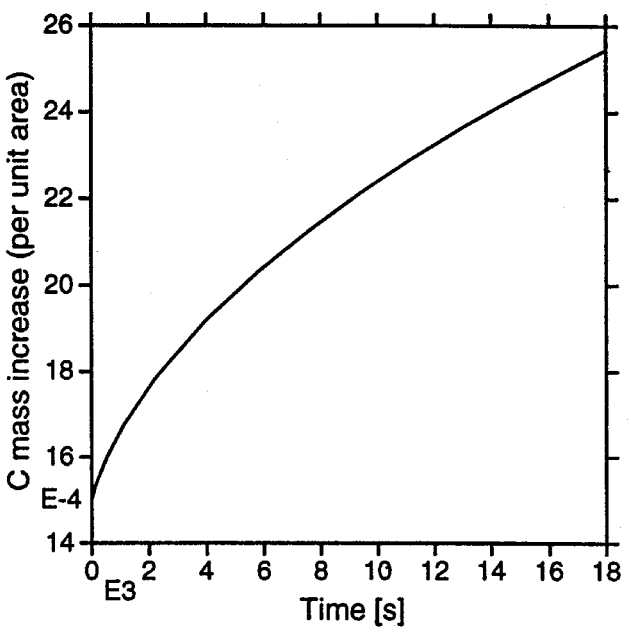


**Fig. 3** Mass increase due to the carburization

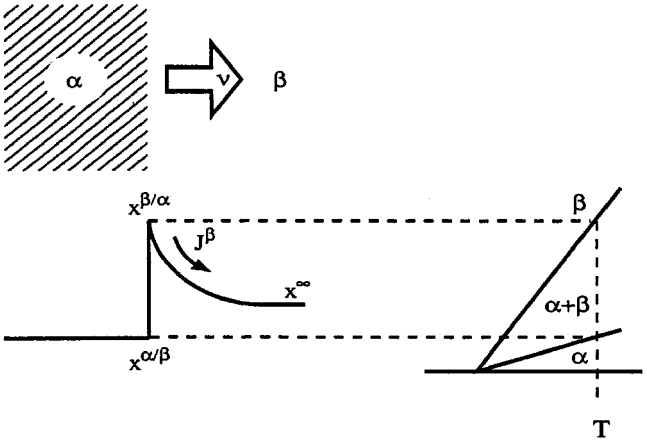


**Fig. 4** The $\alpha$ phase growing into $\beta$ in a binary system under isothermal conditions. The corresponding concentration profile is shown in the lower left part of the figure and the phase diagram in the lower right part of the figure

where $\nu^{\alpha}$ denotes the interface migration rate, $x_k^{\alpha}$ and $x_k^{\beta}$ are the contents of component $k$ in $\alpha$ and $\beta$ close to the phase interface, and $J_k^{\alpha}$ and $J_k^{\beta}$ are the corresponding diffusional fluxes. The term $V_m^{\alpha}$ is the molar volume of the $\alpha$ phase.

The integration in time is carried out by initially calculating the boundary conditions at the phase interface. If the interfacial reactions are fast, compared to the migration of the phase interface, then thermodynamic equilibrium can be assumed to hold locally at the interface. This assumption, usually referred to as the local equilibrium hypothesis, is commonly applied and allows the boundary conditions to be determined. The diffusion problem in each single-phase region can then be solved. Finally, the migration rate of the phase interface is determined by solving the flux-balance

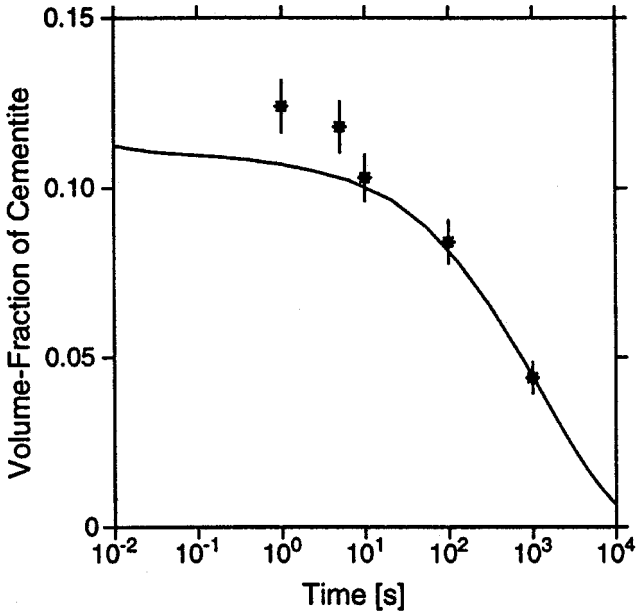


**Fig. 5** The calculated volume fraction of cementite as a function of time, during austenitization of an Fe-2.06 at.% Cr-3.91 at.% C alloy at 910 °C

equation (Eq 15). In the multicomponent case, this will generate a system of nonlinear equations, which have to be solved by an iterative procedure.

The local equilibrium hypothesis implies that there is no difference in chemical potential across the phase interface and that the concentration of the components can be evaluated from phase diagram information. The rate of transformation is then only controlled by the transport of the components to and from the interface. This assumption is a simplification, which disregards many other possible effects present during a phase transformation, *e.g.*, effects from curved interfaces, finite mobility of the interface, solute drag, and elastic stresses. These effects may cause a deviation from the local equilibrium.

Examples of problems, which have been treated with this model, are

- austenite/ferrite diffusional transformations in steels [1982Ågr1, 1990And, 1992Ågr, 1992Crul,
- carbide dissolution during austenitization of steel [1990And, 1991Liu, 1992Ågr],
- certain aspects of solidification [1998Lip],
- nitriding of steels [1995Du1, 1995Du2, 1996Du],
- nitrocarburizing of steels [1996Du], and
- growth or dissolution of intermediate phases in alloy compounds [1995Du2].

**Cementite Dissolution in an Fe-Cr-C Alloy.** Cementite dissolution during austenitization at 910 °C of a soft-annealed Fe-2.06 at.% Cr-3.91 at.% C alloy has been simulated by regarding an average cementite particle in an austenitic matrix. The cementite particle was assumed spherical and the initial particle size was set equal to the average particle size from the soft-annealed state. In Fig. 5, how the cementite

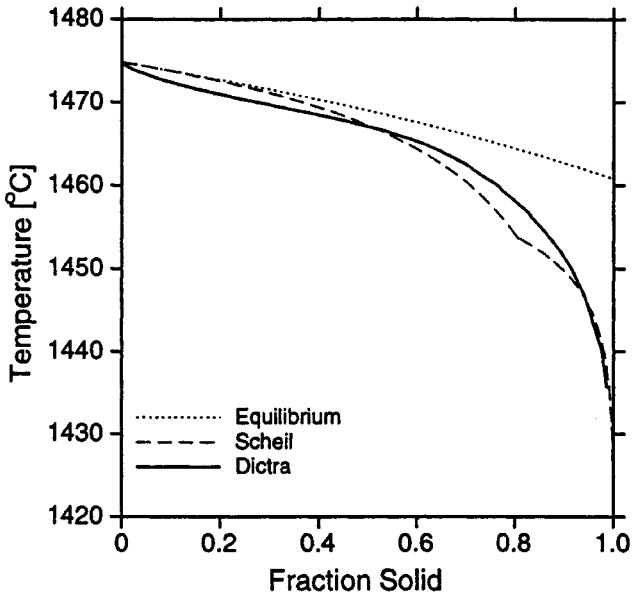


**Fig. 6** Calculated solidification path (solid line) for an Fe-18 mass.% Cr-8 mass.% Ni alloy. The cooling rate in the simulation was 1 K/s and the size of the system was 100 $\mu$m. The results from a Scheil-Gulliver simulation (dashed line) and equilibrium solidification (dotted line) are also shown

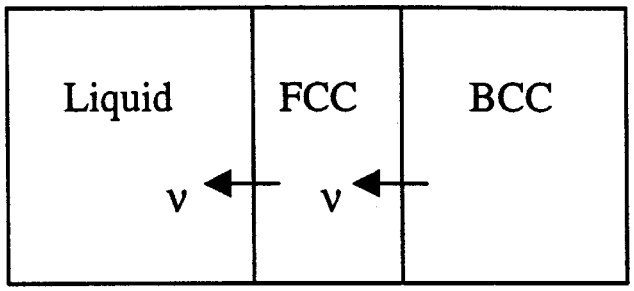


**Fig. 7** The geometry used in the solidification simulation presented in Fig. 6 corresponding to a peritectic reaction. It is also possible to simulate a eutectic reaction in a similar way by adding the solid phases on either side of the liquid phase

particle shrinks as a function of time is shown; the result of the simulation is shown by the solid line [1991Liu] and the symbols denote metallographic measurements.

**Solidification Path of a Fe-18%Cr-%Ni alloy.** Although DICTRA only works with simple geometries, it may be applied to illuminate some aspects of solidification. A solidification path for an Fe-18 mass.% Cr-8 mass.% Ni alloy calculated by DICTRA is shown in Fig. 6. In the simulation, several assumptions had to be made. The cooling rate had to be given *a priori*, as well as the size of the system, which represents half the interdendritic distance. In the beginning of the simulation, only one region containing the liquid phase is present, whereas after some time, three regions are present according to Fig. 7. When a phase becomes stable, a new region will automatically be added to the system. At the end of the simulation when all the liquid has solidified, only two regions remain.

Instead of the cooling rate the amount of heat extracted from the system per time unit can be given. This may in some cases yield a more realistic result since the heat of formation is allowed to affect the cooling rate. The discrepancy between DICTRA and the Scheil simulation at high temperatures is caused by finite diffusion rate in the liquid and at low temperatures by finite diffusion rate in the solid phases, which is taken into account by DICTRA.

### *4.3 Model for Diffusion in Dispersed Systems*

The model for diffusion in dispersed systems was initiated in order to treat some problems for which the previous models were not well suited [1994Eng2]; for example, carburization of high-temperature alloys, where long-range diffusion of carbon occurs in an austenitic matrix with dispersed carbides.

In this model, it is assumed that there exists a continuous phase, the matrix phase, in which there are one or more dispersed phases. Diffusion is assumed to take place only in the matrix phase. The dispersed phases act as point sinks or sources of solute atoms in the simulation and their fraction and composition are calculated from the average composition in each node, assuming that equilibrium holds locally.

The calculation scheme is described in Fig. 8 and consists of two steps. The first step is the so-called diffusion step, which is simply a single-phase problem since it is assumed that all diffusion occurs in a matrix phase. However, due to the composition change in the matrix during the diffusion step, there is a change in the average composition at every node. The new equilibrium is calculated from the new average composition using Thermo-Calc, and the diffusion step is then repeated with the new composition profile in the matrix phase, *etc.*

This model is suitable to any application where long-range diffusion occurs in a single continuous phase containing dispersed particles. Here, "long range" means distances that are long compared to the interparticle spacing. This model is thus not well suited for problems involving rapid temperature changes.

Examples of applications for this model are

- carburization of high-temperature alloys [1994Eng1, 1994Eng2],
- interdiffusion in composite materials [1994Eng2, 1997Hel1, 1997Hel2], and
- gradient sintering of cemented carbide work-tool pieces.

**Carburization of High-Temperature Alloys.** Metals and alloys are generally susceptible to carburization when exposed to an environment containing CO, $CH_4$, or other hydrocarbon gases, such as $C_3H_8$, at elevated temperatures. In the petrochemical industry, as well as in heat treating facilities, several examples of components exposed to such an environment may be found [1990Lai]. The alloys commonly used in these applications contain 15 to 30% Cr for oxidation resistance and improved mechanical properties. Carburization attack on these alloys generally results in the formation of internal Cr-rich carbides, which often cause the alloy to suffer embrittlement, as well as degradation of other mechanical properties [1978Sch]. During carburization of these

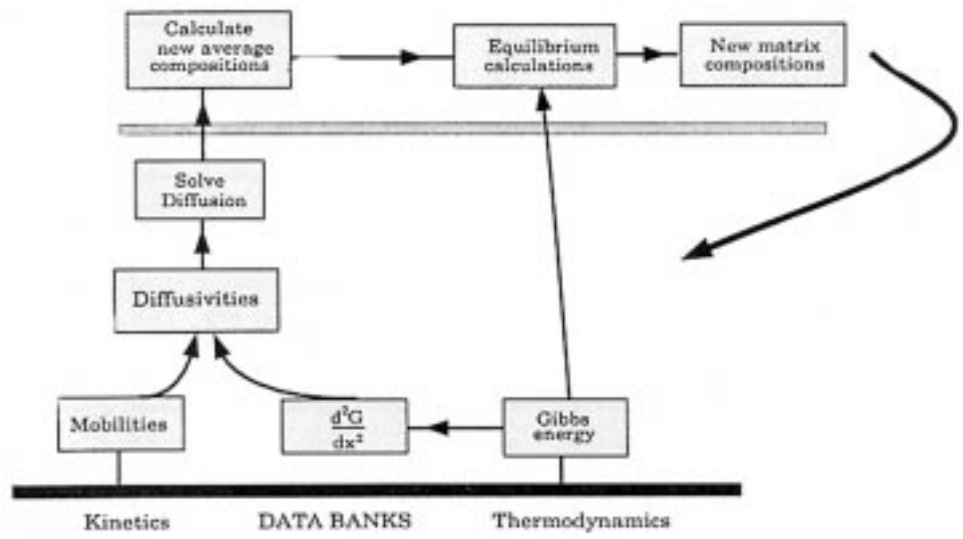


**Fig. 8** The calculation scheme used in the model for diffusion in dispersed systems [1996Eng2]

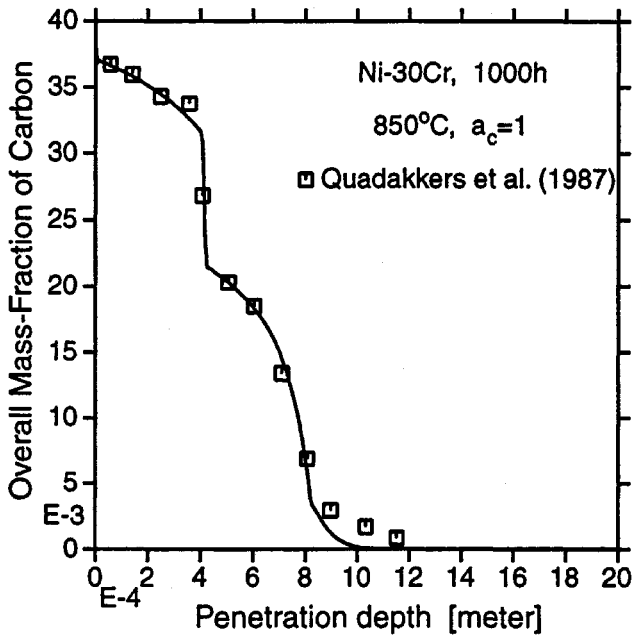


**Fig. 9** Total carbon concentration in mass fraction vs penetration depth for Ni-30 mass. % Cr alloy after carburization for 1000 h at 850 °C with a constant surface carbon activity, $a_c$ = 1. The solid line is calculated, whereas the symbols represent experimental data [1994Eng2]

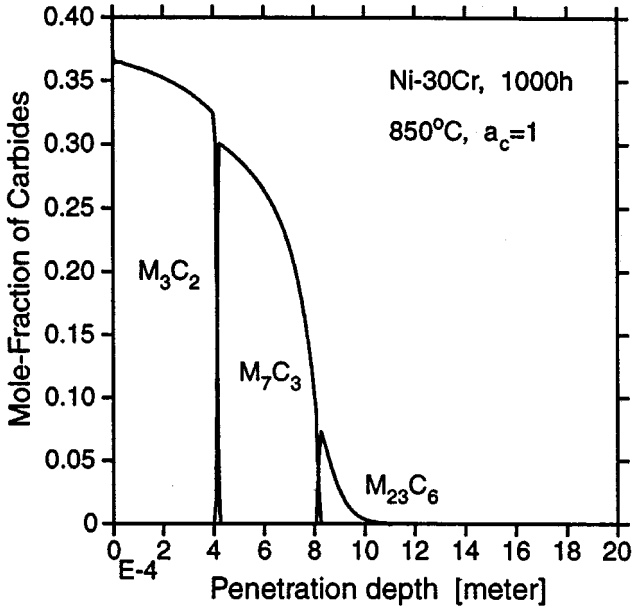


**Fig. 10** Mole fraction of the precipitated carbides vs penetration depth for the Ni-30 mass. % Cr alloy in Fig. 9 [1994Eng2]

alloys, carbon will diffuse in a matrix with dispersed carbide particles and thus the model for diffusion in dispersed systems is well suited for this problem.

The simulated C-concentration profile and the amount of carbides formed during carburization of a Ni-30 mass.% Cr alloy for 1000 h at 850 °C are shown in Fig. 9 and 10, respectively [1994Eng2]. The blocking of the diffusion path by the dispersed carbides was taken into account by multiplying the diffusivities with a so-called labyrinth factor equal to $(f^m)^2$, $f^m$ being the volume fraction of the matrix phase.

**Carbon Diffusion during Annealing of Dissimilar Alloy Weldments.** Weldments between different kinds of heat-resistant steels are commonly used in steam power generating plants. During postweld heat treatment (PWHT), or in service of these weldments, microstructural changes occur due to the difference in chemical potential of carbon between the two steels. The carbon diffusion, which occurs due to this difference, causes a depletion of carbon in the low-alloy steel and formation of a carbide seam in the higher alloyed steel. The depleted zone in the low-alloy steel, heat-affected zone, influences the creep rupture behavior, whereas the carbide seam strongly affects the toughness of the weldment [1989Buc]. It is thus desirable to predict these changes by simulation. A simulated C-concentration profile and the amount of carbides

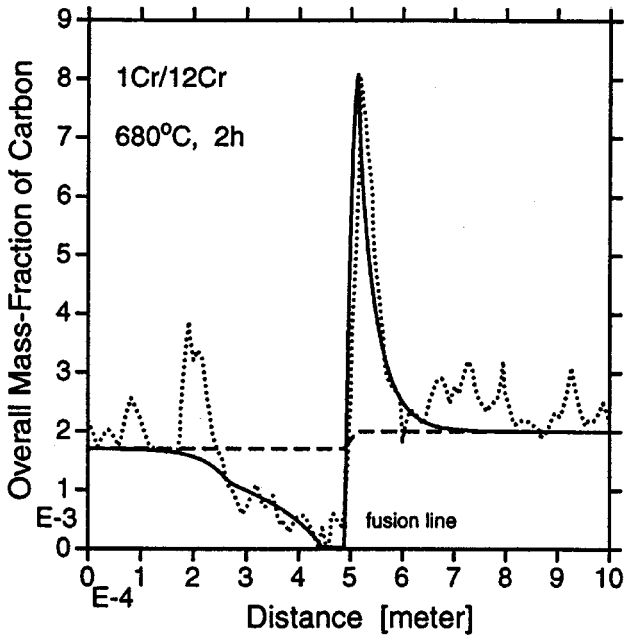


**Fig. 11** Calculated profile (solid line) of total carbon concentration in a 1 mass.% Cr/12 mass.% Cr couple after PWHT at 680 °C for 2 h compared with experiments (dotted line) [1994Eng2]

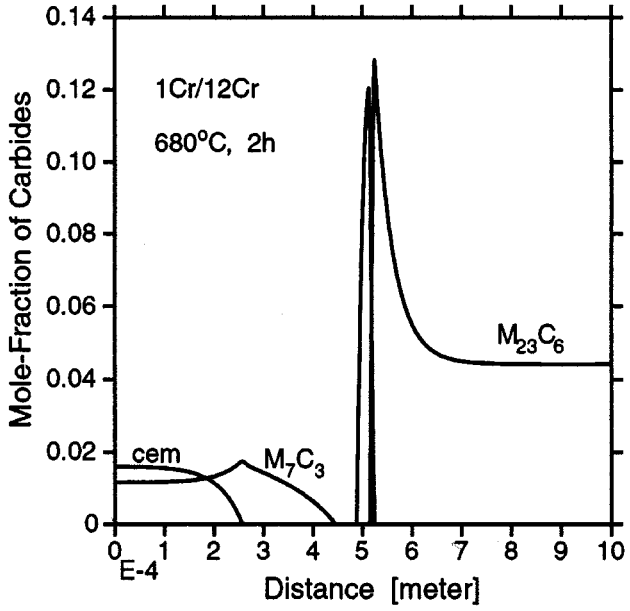


**Fig. 12** Mole fraction of carbides in the weldment after PWHT at 680 °C for 2 h [1994Eng2]

present after 2 h of PWHT at 680 °C for a Fe-1 mass.% Cr/Fe-12 mass.% Cr couple are shown in Fig. 11 and 12, respectively. The agreement between calculation and measurement should be considered as satisfactory. Also, in this case, a labyrinth factor equal to $(f^m)^2$ was used.

### *4.4 Effective Diffusion Model*

The effective diffusion model [1996Eng3] was developed to handle problems with long-range diffusion where it is difficult to distinguish a matrix phase or where different matrix phases prevail in different parts of the material.

The approach taken in this model is to consider a multiphase alloy and divide it into small volume elements, which are large enough to be statistically homogeneous. Each volume element is substituted with an effective phase, having the average composition of the volume element. Equation 4 is rewritten in order to express the total flux, $J_k^{\text{tot}}$, in this effective phase; *i.e.*,

$$J_k^{\text{tot}} = -\sum_{i=1}^{n} L_{ki}^{\text{tot}} \frac{\partial \mu_i}{\partial z} \qquad \text{(Eq 16)}$$

where the $L_{ki}^{'\text{tot}}$ term is some parameter relating the total flux of $k$ to the driving forces. In general, it will be difficult to find experimental data in multiphase alloys from which the $L_{ki}^{'\text{tot}}$ can be calculated and it will thus be necessary to somehow estimate $L_{ki}^{'\text{tot}}$ from $L_{ki}^{'\alpha}$ of the individual phases. One way for such estimations is to apply rules of mixture. Such rules can be found in the literature [1935Bru, 1967Bee, 1976Hal, 1976Pro, 1986Gri] for determining effective transport properties in multiphase mixtures from the transport properties of the individual phases, the fraction of the phases, and perhaps also from information on their geometrical distribution.

As in the single-phase case, it is generally more convenient to express the fluxes as functions of concentration gradients rather than gradients in chemical potential; *i.e.*,

$$J_k^{\text{tot}} = -\sum_{j=1}^{n-1} D_{kj}^{n,\text{tot}} \frac{\partial c_j^{\text{tot}}}{\partial z} \qquad \text{(Eq 17)}$$

This equation, substituted in Eq 2, constitutes a system of coupled PDEs, which can be solved applying a similar procedure as in the single-phase model. However, the large discontinuous change in the effective diffusivities, which occur at some phase boundaries, can cause convergence problems during the numerical integration of the PDEs. In order to avoid this difficulty, it seems necessary to use implicit time integration and evaluate the effective diffusivities at the previous time-step.

The effective diffusion model seems to be able to handle most problems that can be treated with the model for diffusion in dispersed systems, as well as similar problems where no single continuous phase can be identified:

- interdiffusion in composite materials [1997Eng], and
- carburization of high-temperature alloys.

**Interdiffusion in a Multiphase Fe-Cr-Ni Diffusion Couple.** When an Fe-24.3 mass.% Cr-6.9 mass.% Ni alloy is put together with an Fe-40 mass.% Cr-29.4 mass.% Ni alloy in a so-called diffusion couple and annealed at 1100 °C, we have a situation where it is not possible to distinguish a continuous matrix phase throughout the entire composite. The $\alpha$ phase, bcc, is the majority phase and the $\gamma$ phase, fcc, is the secondary phase in the Fe-24.3% Cr-6.9% Ni alloy, whereas the reverse situation is prevalent in the Fe-40%Cr-29.4% Ni alloy. This case was studied experimentally by

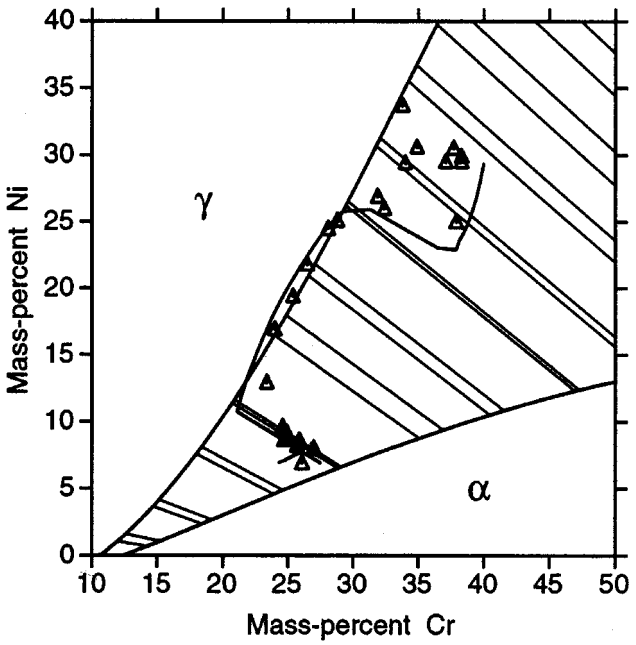


**Fig. 13** Calculated diffusion path for the Fe-24.3 mass.% Cr-6.9 mass.% Ni/Fe-40 mass.% Cr-29.4 mass.% Ni composite after annealing at 1100 °C for 100 h. Symbols are experimental data points from Engström [1995Eng]

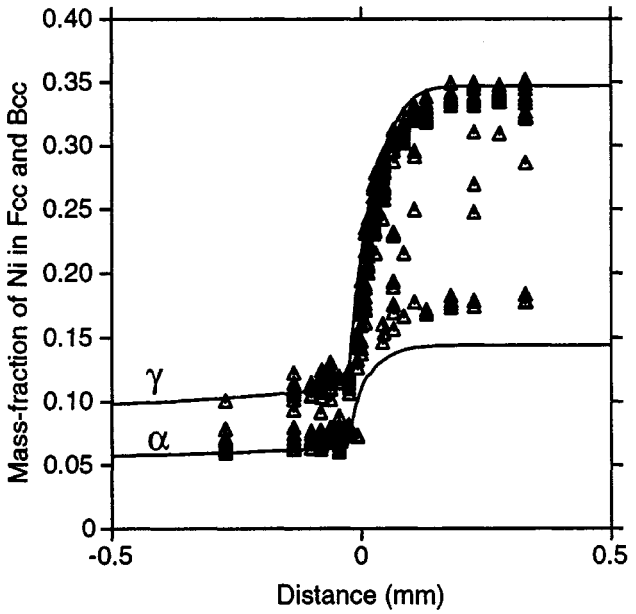


**Fig. 14** Calculated concentration profiles for Ni in the $\alpha$ and $\gamma$ phases after 100 h at 1100 °C. Experimental data points are individual EDS measurements from Engström [1995Eng]

Engström [1995Eng]. It was found that the diffusion path left the $\alpha + \gamma$ two-phase region and a single-phase $\gamma$ layer formed in the middle of the composite. Later, this case was analyzed with the effective diffusion model, and it was found that the model could actually predict the interdiffusion behavior observed in the composite rather well; *e.g.*, the formation of a single-phase $\gamma$ layer was correctly predicted by the calculation [1997Eng]. In the calculation, the familiar Wiener bounds [1912Wie], or more precisely Eq. 4 and 5 in [1996Eng3], were used in order to estimate the kinetic parameters of the effective phase from the kinetic parameters of the $\alpha$ and $\gamma$ phases. The transformation was assumed to occur for a volume fraction equal to 0.5. That is, whenever the volume fraction of the $\gamma$ phase was larger than 0.5, the lower bound was used; otherwise, the upper bound was used. The calculated diffusion path is presented in Fig. 13 together with experimental data points from Engström [1995Eng]. The calculated path leaves the two-phase region and enters the $\gamma$ one-phase region and thus predicts a single-phase $\gamma$ layer. The calculated concentration profiles for Ni in the $\alpha$ and $\gamma$ phases, respectively, are presented in Fig. 14, together with experimental data points from Engström [1995Eng].

### *4.5 The Cell Model*

All models discussed so far consider one cell. However, it is possible to consider two or more such cells interconnected under the assumption of diffusional equilibrium between the cell boundaries and there are thus no differences in diffusion potentials between the cells. A cell contains one or several regions in which the diffusion problem is to be solved. The size of a cell is fixed during the entire simulation, whereas the size of a region may grow or shrink. Two neighboring regions are separated by a mobile interface. The interface at the outer boundary of the cell is immobile, except for such changes caused by volume differences between the phases. The conditions at the inner interface are determined by the local equilibrium assumption, whereas the conditions at the outer interface are determined by the method in which the cells are coupled.

The coupling between the cells is achieved by requiring that the cells at their common boundaries have the same activities for each one of the components and by requiring that the total amount of each component is constant. In order to maintain the overall mass balance, the net flux between the cells is assumed to be zero. The activity will then be iteratively determined until such an activity is found that will yield a zero net sum of fluxes.

This model has been applied to study the escape of carbon from a plate of ferrite assuming that the plate initially formed by a partitionless reaction from an Fe-C austenite [1993Hil]. It is also possible to consider

- dissolution of a particle distribution and
- dissolution of several different types of particles.

### *4.6 The Model for Coarsening*

This model was developed in order to treat coarsening, *i.e.*, Ostwald ripening [1998Gus]. It uses the assumption that coarsening of a system can be described by performing calculations on a single particle of maximum size at the center of a spherical cell. It is assumed that the particle size distribution obeys the Lifshitz-Slyozov-Wagner distribution [1959Lif, 1961Lif, 1961Wag], *i.e.*, that the maximum particle size is

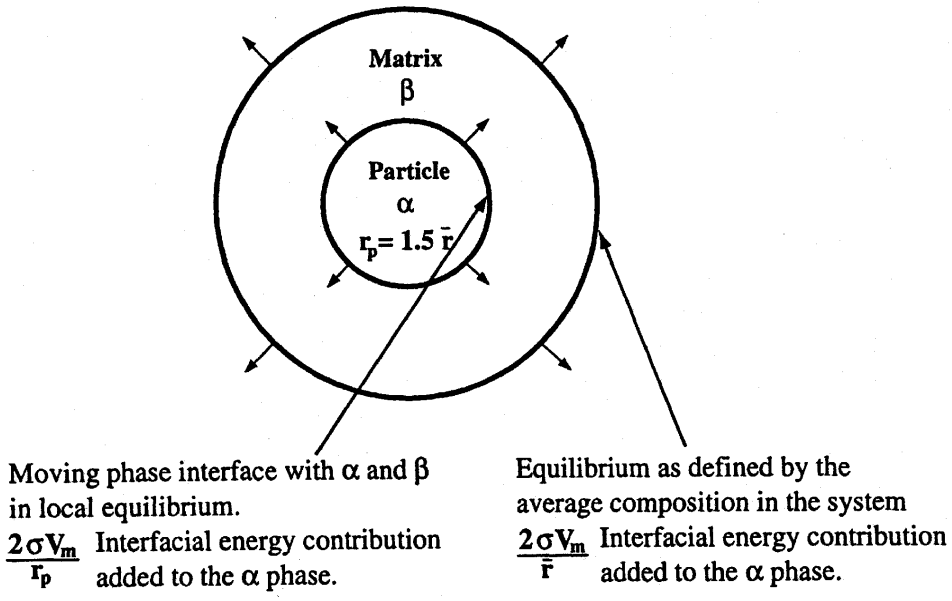


**Fig. 15** A schematic picture of the coarsening model [1998Gus]

1.5 times the average size. In this model, a contribution from the interfacial energy is added to the Gibbs energy function for the particle (Fig. 15),

$$\Delta G_m = \frac{2\sigma V_m}{r} \qquad \text{(Eq 18)}$$

where $\sigma$ is the interfacial energy, $r$ is the particle radius, and $V_m$ is the molar volume. It is assumed that equilibrium between average size particles and the matrix holds locally at the cell boundary, taking into account the contribution of the interfacial energy in Gibbs energy. The particle of the maximum size will have a smaller Gibbs energy addition than the particles of average size, giving a difference in composition from close to the interface between the maximum particle and matrix to the outer cell boundary. This difference will make the maximum particle grow. In order to maintain the total composition in the cell, the size of the cell will increase accordingly.

Examples where this model can be used are

- coarsening of $\gamma'$ particles [1998Gus],
- coarsening of carbides in austenite, and
- coarsening of carbonitrides in ferrite.

**Coarsening of $\gamma'$ Particles in Ternary Ni-Al-Mo Alloys.** Coarsening of $\gamma'$ particles in a Ni-rich matrix in three different Ni-Al-Mo alloys at 872 °C has been simulated and plotted as the cube of the radius as a function of time (Fig. 16) [1998Gus]. Unfortunately, the thermodynamic description used here, the only one available, is not in good agreement with this particular set of experimental observations. In this calculation, the alloy composition was adjusted in order to have the same fraction of $\gamma'$ as observed experimentally. This gave a small difference in composition compared with the experimental data.

### 4.7 The Cooperative Growth Model

The cooperative growth model was developed to simulate the reaction $\gamma \rightarrow \alpha + \beta$, where $\alpha$ and $\beta$ grow cooperatively as lamellar aggregates into a $\gamma$ matrix in both binary and multicomponent alloys [1992Jön].

In this model, the theory for boundary and volume diffusion-controlled lamellar growth of eutectics and eutectoids, as presented by Hillert [1971Hil], has been modified to handle mixed boundary and volume diffusion control for treating growth of lamellar phases, *e.g.*, growth of pearlite in steels. This has been achieved by introducing so-called effective diffusion coefficients. Substitutional alloying elements are here assumed to redistribute by boundary diffusion.

Several assumptions have been made. A steady-state growth rate controlled by diffusion in front of the aggregate was assumed. All diffusivities were assumed independent of alloying effects and diffusion inside the lamella was assumed negligible. Furthermore, it was assumed that the transformation front is approximately planar and that local equilibrium holds across the $\gamma/\alpha$ and $\gamma/\beta$ interfaces.

This model has been applied on the growth of pearlite in binary and multicomponent systems [1992Jön].

**Pearlite Growth in Ternary Fe-Mn-C Alloys.** During the lamellar growth of pearlite in binary Fe-C alloys, volume diffusion of carbon seems to be rate controlling at high temperatures, while boundary diffusion seems to hold at low temperatures. The pearlite growth has been simulated using the model for mixed boundary and volume diffusion-controlled growth for two different 1 mass.% Mn alloys and one 1.8 mass.% Mn alloy (Fig. 17 and 18). Above 600 °C, the temperature versus growth rate curves are in fair agreement

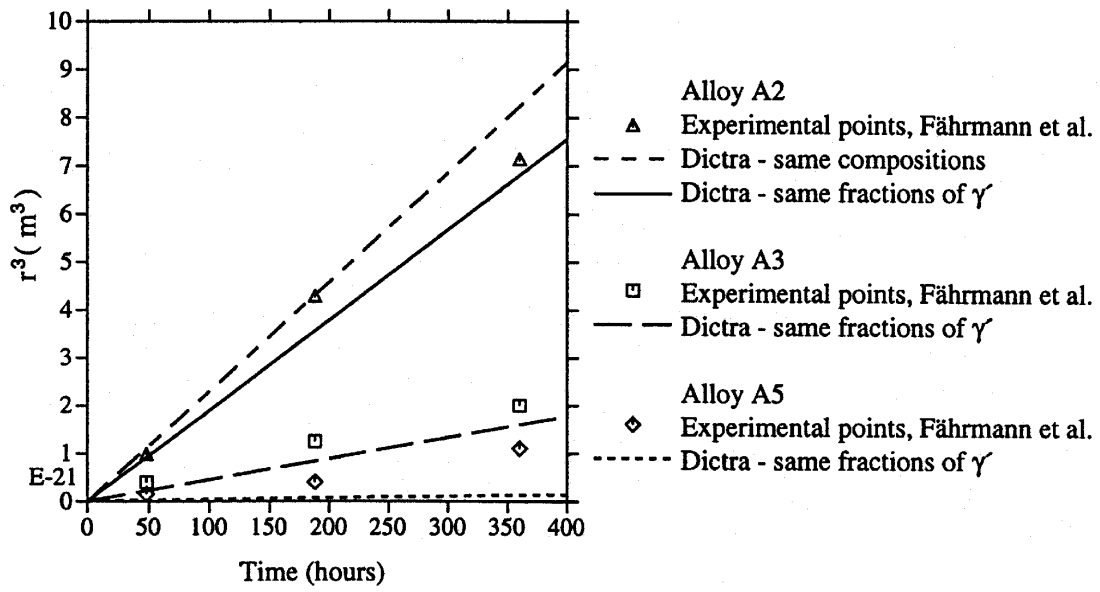


**Fig. 16** Comparison of the coarsening model with experimental data from Fährmann *et al.* [1997Fäh]. Coarsening of $\gamma'$ particles in Ni-Al-Mo at 872 °C is considered [1998Gus]

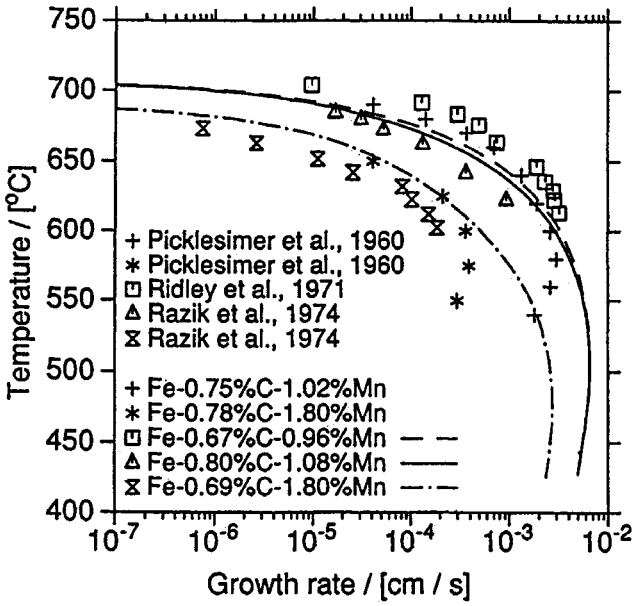


**Fig. 17** Calculated growth rate of pearlite for three ternary Fe-Mn-C alloys. Symbols are experiments from various authors [1992Jön]

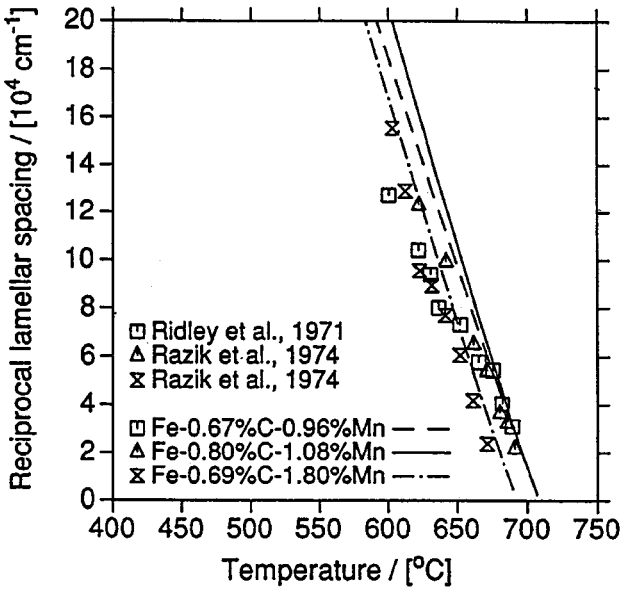


**Fig. 18** Calculated reciprocal lamellar spacing of pearlite for three ternary Fe-Mn-C alloys. Symbols are experiments from various authors [1992Jön]

with the experiments. Below this temperature, the deviation is more pronounced.

## 5. Summary

DICTRA is a software package for simulation of diffusional reactions in multicomponent alloys. It is an engineering tool used daily by engineers and scientists all over the world, allowing simulations to be performed with realistic conditions for alloys of practical importance. It gives a possibility of bringing new insight into problems by linking fundamental models to critically assessed thermodynamic and kinetic data.

This paper gives a brief description of the DICTRA software and the different models included together with some examples on applications. The models in DICTRA are the single-phase model, the moving boundary model, the model for diffusion in dispersed systems, the effective diffusion model, the cell model, the model for coarsening, and the cooperative growth model. It has been demonstrated how the use of various models in DICTRA may yield valuable insight

into and a unique capability to accurately predict important aspects of structural changes during processing and usage of metallic materials.

## References


**1912Wie:** O. Wiener: *Abhandlungen der Mathematisch-Physischen Klasse der Königlichen Sächsischen Gesellschaft der Wissenschaften*, 1912, vol. 32, pp. 509-604.

**1931Ons:** L. Onsager: *Phys. Rev.*, 1931, vol. 37, pp. 405-26; 1931, vol. 38, pp. 2265-79.

**1935Bru:** D.A.G. Bruggeman: *Ann. Phys.*, 1935, vol. 24, pp. 636-79.

**1942Dar:** L.S. Darken: *Trans. AIME*, 1942, vol. 150, pp. 157-71.

**1949Dar:** L.S. Darken: *Trans. AIME*, 1949, vol. 180, pp. 430-38.

**1959Lif:** I.M. Liftshitz and V.V. Slyozov: *Sov. Phys. JETP*, 1959, vol. 35, pp. 331-39.

**1961Lif:** I.M. Liftshitz and V.V. Slyozov: *Chem. Solids*, 1961, vol. 19, pp. 35-50.

**1961Wag:** C. Wagner: *Z. Elektrochemie*, 1961, vol. 65, pp. 581-91.

**1967Bee:** L.K.H. van Beek: *in Progress in Dielectrics*, J.B. Birks, ed., Heywood, London, 1967, vol. 7, pp. 69-113.

**1970Kau:** L. Kaufman and H. Bernstein: *Computer Calculations of Phase Diagrams*, Academic Press, New York, NY, 1970.

**1971Gup:** P.K. Gupta and A.R. Cooper: *Physica*, 1971, vol. 54, pp. 39-59.

**1971Hil:** M. Hillert: *Acta Metall.*, 1971, vol. 19, pp. 769-78.

**1976Hal:** D.K. Hale: *J. Materials Science*, 1976, vol. 11, pp. 2105-41.

**1976Pro:** R.C. Progelhof, J.L. Throne, and R.R. Ruetsch: *Polymer Eng. Sci.*, 1976, vol. 16, pp. 615-25.

**1977Luk:** H.L. Lukas, E.T. Henig, and B. Zimmermann: *CALPHAD*, 1977, vol. 1, pp. 225-36.

**1977Zie:** O.Z. Zienkiewizc: *The Finite Element Method*, 3rd ed., McGraw-Hill, London, 1977.

**1978Sch:** A. Schnaas and H.J. Grabke: *Werkst. Korros.*, 1978, vol. 29, pp. 635-44.

**1980Bon:** K. Bongartz, D.F. Lupton, and H. Schuster: *Metall. Trans. A*, 1980, vol. 11A, pp. 1883-93.

**1982Ågr1:** J. Ågren: *Acta Metall.* 1982, vol. 30, pp. 841-51.

**1982Ågr2:** J. Ågren: *J. Phys. Chem. Solids*, 1982, vol. 43, pp. 385-91.

**1984Jan:** B. Jansson: Internal Report, Trita-Mac-234, Division of Physical Metallurgy, Royal Institute of Technology, Stockholm, 1984.

**1985Sun:** B. Sundman, B. Jansson, and J.-O. Andersson: *CALPHAD*, 1985, vol. 9, pp. 153-90.

**1986Gri:** G. Grimvall: *Thermophysical Properties of Materials*, North-Holland, Amsterdam, 1986, pp. 257-83.

**1989Bon:** K. Bongartz, W.J. Quadakkers, R. Schulten, and H. Nickel: *Metall. Trans. A*, 1989, vol. 20A, pp. 1021-28.

**1989Buc:** B. Buchmayr, H. Cerjak, J.S. Kirkaldy, and M. Witwer: *2nd Int. Conf. Trends in Welding Research*, Gatlinburg, TN, 1989, ASM International, Materials Park, OH, 1990, pp. 237-42.

**1990And:** J.-O. Andersson, L. Höglund, B. Jönsson, and J. Ågren: in *Fundamentals and Applications of Ternary Diffusion*, G.R. Purdy, ed., Pergamon Press, New York, NY, 1990, pp. 153-63.

**1990Lai:** G.Y. Lai: *High-Temperature Corrosion of Engineering Alloys*, ASM International, Materials Park, OH, 1990.

**1991Liu:** Z.-L. Liu, L. Höglund, B. Jönsson, and J. Ågren: *Metall. Trans. A*, 1991, vol. 22A, pp. 1745-52.

**1992And:** J.-O. Andersson and J. Ågren: *J. Appl. Phys.*, 1992, vol. 72, pp. 1350-55.

**1992Cru:** S. Crusius, L. Höglund, G. Inden, U. Knoop, and J. Ågren: *Z. Metallkd.*, 1992, vol. 83, pp. 729-38.

**1992Jön:** B. Jönsson: Internal Report, Trita-Mac-478, Division of Physical Metallurgy, Royal Institute of Technology, Stockholm, 1992.

**1992Mor:** J.E. Morral, B.M. Dupen, and C.C. Law: *Metall. Trans. A*, 1992, vol. 23A, pp. 2069-71.

**1992Ågr:** J. Ågren: *Iron Steel Inst. Jpn. Int.*, 1992, vol 32, pp. 291-96.

**1993Hil:** M. Hillert, L. Höglund, and J. Ågren: *Acta Metall. Mater.*, 1993, vol. 41, pp. 1951-57.

**1994Engl:** A. Engström, L. Höglund, and J. Ågren: *Mater. Sci. Forum*, 1994, vol. 163-165, pp. 725-30.

**1994Eng2:** A. Engström, L. Höglund, and J. Ågren: *Metall. Mater. Trans. A*, 1994, vol. 25A, pp. 1127-34.

**1994Jönl:** B. Jönsson: *Z. Metallkd.*, 1994 vol. 85, pp. 498-501.

**1994Jön2:** B. Jönsson: *Z. Metallkd.*, 1994 vol. 85, pp. 502-09.

**1994SGT:** *SGTE (Scientific Group Thermodata Europé) Solution Database of Jan. 1994*, B. Sundman, ed., Division of Computational Thermodynamics, Royal Institute of Technology, S-100 44 Stockholm, Sweden, e-mail: bosse@met.kth.se.

**1995Dul:** H. Du and J. Ågren: *Z. Metallkd.*, 1995, vol 86, pp. 522-29.

**1995Du2:** H. Du, N. Lange, and J. Ågren: *Surf. Eng.*, 1995, vol. 11, pp. 301-08.

**1995Eng:** A. Engström: *Scand. J. Metall.*, 1995, vol. 24, pp. 12-20.

**1995Jön:** B. Jönsson: *Iron Steel Inst. Jpn. Int.*, 1995, vol. 35, pp. 1415-21.

**1996Du:** H. Du and J. Ågren: *Metall. Mater. Trans. A*, 1996, vol. 27A, pp. 1073-79.

**1996Eng1:** A. Engström and J. Ågren: *Z. Metallkd.*, 1996 vol. 87, pp. 92-97.

**1996Eng2:** A. Engström: Ph. D. Dissertation, Division of Physical Metallurgy, Royal Institute of Technology, Stockholm, 1996.

**1996Eng3:** A. Engström: Internal Report, Trita-Mac 602, Division of Physical Metallurgy, Royal Institute of Technology, Stockholm, 1996.

**1996Kat:** U.R. Kattner, W.J. Boettinger, and S.R. Coriell: *Z. Metallkd.*, 1996, vol. 87, pp. 522-28.

**1996Ågr:** J. Ågren: *Current Opinion in Solid State & Materials Science*, 1996, vol. 1, pp. 355-60.

**1997Eng:** A. Engström: Division of Physical Metallurgy, Royal Institute of Technology, Stockholm, unpublished results, 1997.

**1997Hell:** T. Helander and J. Ågren: *Metall. Mater. Trans. A*, 1997, vol. 28A, pp. 303-08.

**1997Hel2:** T. Helander, J.-O. Nilsson, and J. Ågren: *Iron Steel Inst. Jpn. Int.*, 1997, vol. 37, pp. 1139-45.

**1997Hög:** L. Höglund: Internal Report Trita-Mac-0605, Division of Physical Metallurgy, Royal Institute of Technology, Stockholm, 1997.

**1997Sau:** N. Saunders: Thermotech Ltd., Guildford, Surrey United Kingdom, personal communications, 1997.

**1998Gus:** Å. Gustafson, L. Höglund, and J. Ågren: *Advanced Heat Resistant Steels for Power Generation*, Conf. Proc. San Sebastian, Spain, Apr. 27-29, 1998, R. Viswananthan and J. Nutting eds., IOM Communications Ltd., Institute of Materials, London, pp. 270-76.

**1998Lip:** H.E. Lippard, C.E. Campbell, T. Björklind, U. Borggren, P. Kellgren, V.P. Dravid, and G.B. Olson: *Metall. Mater. Trans. B*, 1998, vol. 29B, pp. 205-10.

**1998Spr:** L. Sproge and J. Ågren: *J. Heat Treatment*, 1998, vol. 6, pp. 9-19.

**1999Lee:** B.-J. Lee: *Scripta Mater.*, 1999, vol. 40, pp. 573-79.

**1999Ree:** R.C. Reed, M.P. Jackson, and Y.S. Na: *Metall. Mater. Trans. A*, 1999, vol. 30A, pp. 521-33.